

# Measurement and empirical evaluation of acoustic loss in tube with abrupt area change

Yuki Ueda,<sup>1, a)</sup> Shunsuke Yonemitsu,<sup>1</sup> Kenichiro Ohashi,<sup>1</sup> and Takuya Okamoto<sup>1</sup>

*Graduate school of Bio-Applications and Systems Engineering,*

*Tokyo University of Agriculture and Technology, 2-24-16 Nakacho, Koganei,*

*Tokyo 184-8588, Japan*

(Dated: 9 December 2019)

1 This study measures the acoustic power loss that occurs when an acoustic wave passes  
2 through a tube with an abrupt change in area. It is determined that the power loss  
3 is proportional to the third power of the velocity amplitude, and that the propor-  
4 tionality coefficient depends upon the area change ratio of the tube. On the other  
5 hand, the proportionality coefficient is almost independent of the acoustic impedance  
6 and frequency in the 80-250 Hz range. Furthermore, the effect of a tapered tube in  
7 reducing the coefficient is experimentally investigated. Based on these experimental  
8 results, an empirical estimation method for the acoustic power loss is proposed and  
9 validated using a high-pressure-helium-filled tube.

---

<sup>a)</sup>[uedayuki@cc.tuat.ac.jp](mailto:uedayuki@cc.tuat.ac.jp)

## 10 I. INTRODUCTION

11 When fluids flow in tubes, two types of energy loss occur: One is due to the tube length,  
 12 whereas the other is due to geometrical irregularities, such as abrupt area change, bifurcation,  
 13 and bend. The latter is referred to as minor loss.<sup>1-5</sup> For unidirectional fluid flow, both types  
 14 of losses have been investigated and are well documented in several textbooks on fluid  
 15 dynamics. However, for oscillatory fluid flow, only few studies<sup>1-5</sup> have addressed the minor  
 16 loss, although energy loss due to the tube length<sup>7-9</sup> has been well understood.

17 Wakeland and Keolian<sup>3</sup> showed an equation for the acoustic minor loss. This equation is  
 18 based on the Bernoulli equation and is expressed as follows:

$$\Delta W = \frac{2}{3\pi} \rho_m S K |U|^3, \quad (1)$$

19 where  $\Delta W$  is the acoustic minor loss,  $\rho_m$  is the time averaged density of the working gas,  $S$   
 20 is the cross-sectional area of the tube, where the minor loss occurs,  $|U|$  is the peak amplitude  
 21 of the oscillatory velocity averaged over the cross-sectional area of the tube, and  $K$  is the  
 22 coefficient of the minor loss. Hence, the acoustic minor loss can be estimated if the value  
 23 of  $K$  is known. Because  $K$  cannot be theoretically derived, there is a need for empirical  
 24 determination.

25 Abrupt area change generated by the connection of two tubes with different cross-sectional  
 26 areas is one of the most common geometrical irregularities in acoustic systems. Morris et  
 27 al.<sup>4</sup> computationally investigated the acoustic minor loss in a sharp-edged expansion with  
 28 a tube cross-section-area ratio of 0.01, and presented the flow structure at the vicinity of  
 29 the expansion point. Based on this result, the minor loss factor was derived. Smith and

30 Swift<sup>2</sup> experimentally investigated the acoustic minor loss with an infinite area ratio and  
 31 elucidated the effects of a rounded edge at the connecting point. King and Smith, and Doller  
 32 experimentally investigated the effect of a tapered tube on the minor loss, and showed the  
 33 minor loss can be reduced by a tapered tube.<sup>5,6</sup>

34 One of the critical parameters of the abrupt area change is the ratio of the cross-sectional  
 35 areas of the tubes. However, researches on the variation of the area ratio is limited as  
 36 mentioned above. Hence, we evaluate the effect of the area ratio on the minor loss in this  
 37 study. The minor loss is measured by changing the velocity amplitude and area ratio. It is  
 38 confirmed that the minor loss is proportional to the third power of the velocity amplitude,  
 39 as predicted by Eq. (1). The value of  $K$  is experimentally determined as a function of the  
 40 area ratio. In addition, the effect of the acoustic frequency and acoustic impedance, which  
 41 depict the oscillatory flow characteristics, is investigated. Furthermore, following King and  
 42 Smith<sup>5</sup>, and Doller<sup>6</sup> the effect of a tapered tube on the reduction of  $K$  is examined. Finally,  
 43 an empirical equation is introduced for estimating the acoustic minor loss, and validated  
 44 using a high-pressure-helium-filled tube.

## 45 II. EXPERIMENTAL SETUP

46 The schematic of the experimental apparatus is illustrated in Fig. 1. The apparatus  
 47 comprises circular tubes A and B connected to each other at a sharp edge, and a unit  
 48 including a speaker (FW168N, Fostex Co. Ltd.). The cross-sectional areas of tubes A and  
 49 B are denoted by  $S_A$  and  $S_B$ , respectively. Tube A is connected to the speaker unit and two  
 50 pressure sensors (PD-104, JTEKT Co. Ltd.) are mounted on the tube wall. The distance

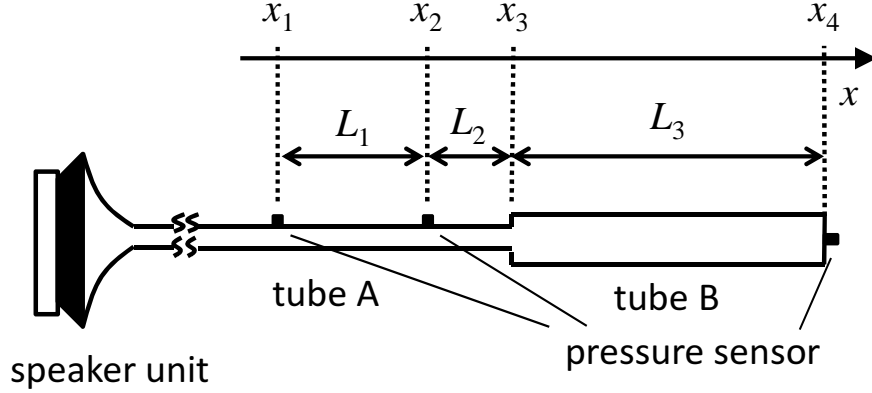


FIG. 1. Schematic of the experimental setup.

51 between the sensors is denoted by  $L_1$ , and the distance between one of the sensors and the  
 52 connecting point (see Fig. 1) is denoted by  $L_2$ . One end of tube B is closed by a brass plate  
 53 on which a pressure sensor (PD-104, JTEKT Co. Ltd.) is mounted. The length of tube B  
 54 is denoted by  $L_3$ . The apparatus is filled with atmospheric air.

55 In this experiment, the value of  $R_{AB} = S_A/S_B$  or its inverse is selected as one of the  
 56 variable parameters. Table I lists the values of the radius  $r_A$  of tube A, radius  $r_B$  of tube  
 57 B, and  $R_{AB}$ . Note that the experiments are performed under two conditions, i.e.  $R_{AB} \leq 1$   
 58 and  $R_{AB} > 1$ .

### 59 III. MEASUREMENT METHOD

60 As shown in Fig. 1, pressure is measured at two points on the wall of tube A and one  
 61 point on the closed end of tube B. This section describes the method for evaluating  $\Delta W$   
 62 using the three measured pressure values. This method is similar to the method used in our  
 63 previous study<sup>10</sup>.

TABLE I. Radii of tube A (top row) and tube B (left column) and the corresponding  $R_{AB}$  values (and  $1/R_{AB}$ ).

$r_A(\text{mm}) \backslash r_B(\text{mm})$	7.5	12	16	20
7.5	1	2.56 (0.39)	4.55 (0.22)	7.11 (0.14)
12	0.39	1	1.78 (0.56)	2.78 (0.36)
16	0.22	0.56	1	1.56 (0.64)
20	0.14	0.36	0.64	1

64 **A. Acoustic power and minor loss**

65 It is assumed that an acoustic field with a single frequency is formed in the circular  
 66 tube, with the  $x$ -axis set along the length of the tube. The tube radius is assumed to be  
 67 considerably smaller than the wavelength of the acoustic wave. For expressing the acoustic  
 68 pressure and cross-sectional mean velocity amplitudes, the complex number  $P(x)$  and  $U(x)$   
 69 are used, respectively. Using  $P(x)$  and  $U(x)$ , the acoustic power, which is the time-averaged

70 rate of acoustic energy transmission through the tube cross-section, is determined as

$$W(x) = \frac{S}{2} \text{Re} \left[ P(x) \tilde{U}(x) \right], \quad (2)$$

71 where notation  $\tilde{\phantom{x}}$  indicates the complex conjugate, and  $S$  is the cross-sectional area of the  
 72 tube. If we denote the acoustic power in front and immediately behind the geometrical  
 73 irregularity by  $W_+$  and  $W_-$ , respectively, the acoustic minor loss can be expressed as

$$\Delta W = W^+ - W^-. \quad (3)$$

74 When acoustic minor loss does not occur,  $W_+ = W_-$ ; hence,  $\Delta W = 0$ .

## 75 B. Theory

76 Based on the linear acoustic theory, the momentum and continuity equations<sup>12,13</sup> for a  
 77 circular tube can be expressed as

$$\frac{dP(x)}{dx} = -\frac{i\omega\rho_m}{1-\chi_\nu}U(x) \quad (4)$$

$$\frac{dU(x)}{dx} = -\frac{i\omega[1+(\gamma-1)\chi_\alpha]}{\gamma P_m}P(x), \quad (5)$$

78 where  $\omega$  is angular frequency, and  $\rho_m$ ,  $P_m$ ,  $\gamma$ , and  $\sigma$  are the mean density, mean pressure,  
 79 specific heat ratio, and Prandtl number of the working gas, respectively.  $\chi_\alpha$  and  $\chi_\nu$  are  
 80 complex functions<sup>12-14</sup> that are denoted below. To express these functions, we use two  
 81 parameters, namely, the thermal relaxation time  $\tau_\alpha$  and viscous relaxation time  $\tau_\nu$ .<sup>14</sup> These  
 82 parameters are defined as

$$\tau_\alpha = r^2/(2\alpha) \quad (6a)$$

$$\tau_\nu = r^2/(2\nu), \quad (6b)$$

83 where  $r$  is the tube radius,  $\alpha$  is the thermal diffusivity of the working gas, and  $\nu$  is its  
 84 kinematic viscosity. For a circular-cross-section tube, functions  $\chi_\alpha$  and  $\chi_\nu$  are expressed  
 85 as<sup>12–14</sup>

$$\chi_\alpha = \frac{2J_1(Y_\alpha)}{Y_\alpha J_0(Y_\alpha)} \quad (7a)$$

$$\chi_\nu = \frac{2J_1(Y_\nu)}{Y_\nu J_0(Y_\nu)}, \quad (7b)$$

86 where

$$Y_\alpha = (i - 1)\sqrt{\omega\tau_\alpha} \quad (8a)$$

$$Y_\nu = (i - 1)\sqrt{\omega\tau_\nu}. \quad (8b)$$

87 Equations (4) and (5) can be solved analytically. With the obtained solution, the pressure  
 88 and cross-sectional mean velocity at  $x = x_b$  can be expressed by those at  $x = x_a$  as<sup>11,15</sup>

$$\begin{pmatrix} P(x_b) \\ U(x_b) \end{pmatrix} = M(x_a, x_b) \begin{pmatrix} P(x_a) \\ U(x_a) \end{pmatrix} \quad (9)$$

89

$$M(x_a, x_b) \equiv \begin{pmatrix} m_{11}(x_a, x_b) & m_{12}(x_a, x_b) \\ m_{21}(x_a, x_b) & m_{22}(x_a, x_b) \end{pmatrix}$$

$$m_{11}(x_a, x_b) = \cos(k(x_b - x_a))$$

$$m_{12}(x_a, x_b) = -iZ_0 \sin(k(x_b - x_a))$$

$$m_{21}(x_a, x_b) = \frac{-i}{Z_0} \sin(k(x_b - x_a))$$

$$m_{22}(x_a, x_b) = \cos(k(x_b - x_a)).$$

90 Here,  $k$  is the complex wave number and  $Z_0$  is the characteristic impedance calculated as

$$k = \frac{\omega}{c} \sqrt{\frac{1 + (\gamma - 1)\chi_\alpha}{1 - \chi_\nu}}, \quad (10)$$

91 and

$$Z_0 = \rho_m \frac{\omega}{k(1 - \chi_\nu)}, \quad (11)$$

92 respectively, where  $c$  is the adiabatic sound speed.

93 First, let us consider the method for evaluating  $W^+$  using the pressure measured at the  
 94 two locations on the wall of tube A. The measuring points are set as  $x_1$  and  $x_2$ , respectively,  
 95 and the junction point is set as  $x_3$ , as shown in Fig. 1. From Eq. (9),

$$U(x_1) = \frac{P(x_2) - m_{11}(x_1, x_2)P(x_1)}{m_{12}(x_1, x_2)}. \quad (12)$$

96 Equation (9) is represented as

$$\begin{pmatrix} P(x_3) \\ U(x_3) \end{pmatrix} = M(x_1, x_3) \begin{pmatrix} P(x_1) \\ U(x_1) \end{pmatrix}, \quad (13)$$

97 and hence,

$$\begin{aligned} \begin{pmatrix} P(x_3) \\ U(x_3) \end{pmatrix} &= M(x_1, x_3) \begin{pmatrix} P(x_1) \\ \frac{P(x_2) - m_{11}(x_1, x_2)P(x_1)}{m_{12}(x_1, x_2)} \end{pmatrix} \\ &= M(x_1, x_3) \begin{pmatrix} 1 & 0 \\ \frac{-m_{11}(x_1, x_2)}{m_{12}(x_1, x_2)} & \frac{1}{m_{12}(x_1, x_2)} \end{pmatrix} \begin{pmatrix} P(x_1) \\ P(x_2) \end{pmatrix}. \end{aligned} \quad (14)$$

98 Substituting  $L_1$  and  $L_2 + L_1$  for  $(x_2 - x_1)$  and  $(x_3 - x_1)$ , respectively, in Eq. (14), we can  
 99 obtain the pressure  $P$  and velocity  $U$  at  $x = x_3$ , i.e. at the junction. With  $P(x_3)$ ,  $U(x_3)$ ,  
 100 and Eq. (2), the acoustic power  $W^+$  at the connecting point tube A is obtained.

101 Next, let us consider the method for expressing the acoustic power  $W^-$  at the connecting  
 102 point of tube B. We set the closed end as  $x_4$ , and modify Eq. (9) as

$$\begin{pmatrix} P(x_3) \\ U(x_3) \end{pmatrix} = M(x_4, x_3) \begin{pmatrix} P(x_4) \\ U(x_4) \end{pmatrix}. \quad (15)$$

103 At the closed end, the velocity becomes zero and the pressure  $P_{closed}$  is measured. Substi-  
 104 tuting  $x_3 - x_4 = -L_3$ ,  $P(x_4) = P_{closed}$ , and  $U(x_4) = 0$  in Eq. (15), we can obtain  $P(x_3)$  and  
 105  $U(x_3)$  at the connecting point of tube B. With  $P(x_3)$ ,  $U(x_3)$ , and Eq. (2), we can calculate  
 106  $W^-$ . It should be noted that the values of  $P(x_3)$  and  $U(x_3)$  for calculating  $W^-$  are not  
 107 equal to the values of  $P(x_3)$  and  $U(x_3)$  for  $W^+$ . Substituting the obtained  $W_+$  and  $W_-$  in  
 108 Eq. (3), we can evaluate the acoustic minor loss  $\Delta W$ .

## 109 IV. RESULTS

### 110 A. Preliminary Experiment

111 To verify the experimental method described in Sec. III, we perform the experiment with  
 112  $R_{AB} = 1$ . Both  $r_A$  and  $r_B$  are set to 7.5 mm, 12 mm, 16 mm, and 20 mm, respectively. The  
 113 lengths  $L_1$  and  $L_2 + L_3$  are set to 390 mm and 750 mm, respectively. The frequency,  $\omega/(2\pi)$ ,  
 114 of the input acoustic wave is maintained at 161 Hz which is the second resonant frequency  
 115 of the gas column in the setup. As a result of the use of the second resonance frequency, the  
 116 velocity antinode appears between  $x_2$  and  $x_4$  rather than in the vicinity of the speaker unit.

117 Although there is no cross-sectional variation, we set a virtual connecting point at the  
 118 velocity antinode and measured  $W^+ - W^-$ ; this is denoted by  $\delta W$ . In Fig. 2, the measured

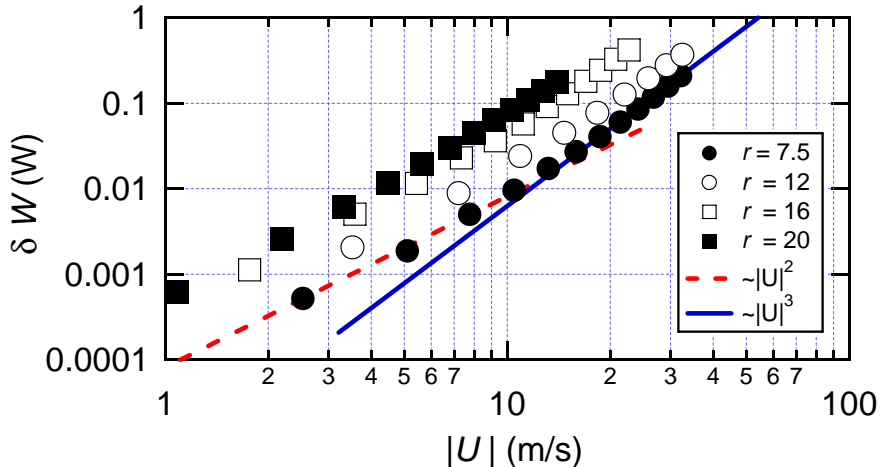


FIG. 2. Measured  $\delta W$  in a straight tube as a function of the velocity amplitude at the velocity antinode.

119  $\delta W$  is depicted as a function of the velocity amplitude  $|U|$ , where the value of  $r$  shown in this  
 120 figure refers to the radius of the circular tube cross-section. Notably, the maximum  $|U|$  for  
 121 each  $r$  shown in Fig. 2 is approximately equal to the maximum  $|U|$  obtained by measuring  
 122  $\Delta W$  described in Sec. IV B. As observed in Fig. 2,  $\delta W$  is nonzero and depends upon  $|U|$  with  
 123  $S = r^2\pi$ , i.e.  $\delta W(U, S)$ . The dotted and solid lines in Fig. 2 show functions proportional to  
 124  $|U|^2$  and  $|U|^3$ , respectively. They indicate that  $\delta W(U, S) \propto |U|^2$  when  $|U| < 10$  m/s, whereas  
 125  $\delta W(U, S) \propto |U|^3$  when  $|U| > 20$  m/s. In addition, the repeatability of the measured value  
 126 of  $\delta W$  was confirmed. We consider that when  $|U| < 10$  m/s, the source of  $\delta W(U, S)$  is  
 127 the underestimation of tube wall attenuation due to the viscosity and thermal conductivity  
 128 of the gas. On the other hand,  $|U| > 20$  m/s,  $\delta W(U, S)$  can be attributed to nonlinearity  
 129 due to the large amplitude of the oscillatory velocity.<sup>16–18</sup> When  $|U|$  is maximized for each  
 130  $r$ , the Reynolds number  $Re_{os}$  determined using  $|U|$  and  $2r$  approaches or just exceeds the  
 131 critical value<sup>17,18</sup> above which flow becomes turbulent. For example, when  $r = 7.5$  mm,

132 the maximum velocity amplitude is 32 m/s, thus,  $Re_{os} = 2.7 \times 10^4$ , while the critical  $Re_{os}$   
 133 estimated by the equation proposed by Merkli and Thoman<sup>18</sup> is  $2.3 \times 10^4$ . Based on these  
 134 preliminary experimental results, we suggest that  $\delta W(U, S)$  represents the additional losses  
 135 occurring in a straight section of the tubes and assume that  $\delta W(U, S)$  is proportional to the  
 136 length of the tube,  $L$ . Instead of Eq. (3), we use

$$\begin{aligned} \Delta W = & (W^+ - \frac{L_1 + L_2}{L_1 + L_2 + L_3} \delta W(U_A, S_A)) \\ & - (W^- + \frac{L_3}{L_1 + L_2 + L_3} \delta W(U_B, S_B)), \end{aligned} \quad (16)$$

137 for measuring  $\Delta W$ , where  $U_A$  and  $U_B$  are  $U(x_3)$  in tube A and tube B, respectively. Note  
 138 that the impact of the additional loss on the value of  $K$  is found to be approximately 0.15

## 139 B. Measurement of the acoustic minor loss

140 In this study, we investigate the effect of three factors on the value of  $K$ : the effect of  
 141 the ratio of the tube cross-sectional area  $R_{AB}$ , absolute value of the acoustic impedance  
 142 ( $|Z| = |P|/|U|$ ), and frequency ( $\omega/(2\pi)$ ).

### 143 1. *Effect of the tube cross-sectional area ratio on the acoustic minor loss coeffi-* 144 *cient*

145 In the experimental setup shown in Fig. 1, the pressure and velocity amplitudes depend  
 146 on position  $x$ . To highlight the effect of the velocity amplitude while minimizing the effect of  
 147 the pressure amplitude, we set the connecting point in the vicinity of the velocity antinode.

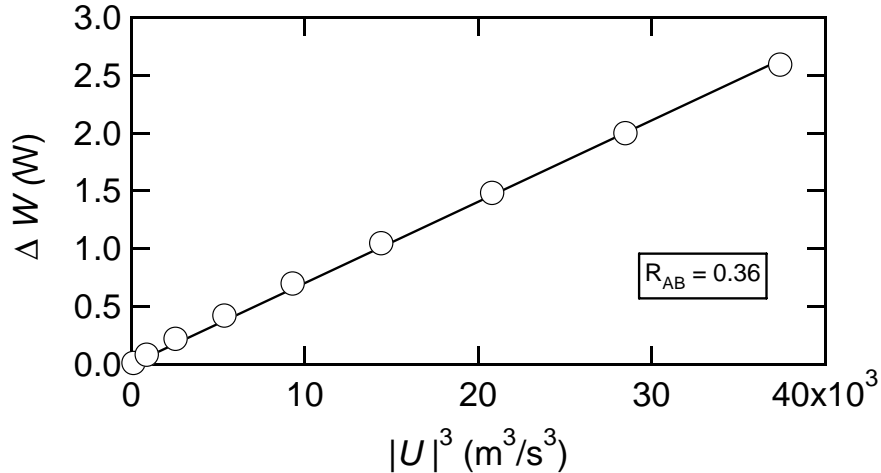


FIG. 3. Measured acoustic minor loss. The radii of tube A and tube B are 12 mm and 20 mm, respectively, resulting in  $R_{AB} = 0.36$ .

148 According to previous research<sup>19</sup>, the velocity amplitude  $|U|$  at the connecting point in the  
 149 narrower tube is used as the representative value.

150 In Fig. 3, the measured  $\Delta W$  is depicted as a function of  $|U|^3$ . The experimental conditions  
 151 are  $\omega/(2\pi) = 161\text{Hz}$ ,  $L_1 = 390$  mm,  $L_2 = 250$  mm,  $L_3 = 500$  mm, and  $R_{AB} = 0.36$  ( $r_A = 12$   
 152 mm and  $r_B = 20$  mm). Figure 3 shows that the value of  $\Delta W$  linearly increases with the  
 153 increase in  $|U|^3$ . When  $|U| = 33.4$  m/s ( $|U|^3 \sim 37000$  m<sup>3</sup>/s<sup>3</sup>),  $\Delta W$  is 2.59 W. This value  
 154 is considerably greater than the  $\delta W$  for straight tubes. (See data indicated by the unfilled  
 155 circle at  $|U| = 33$  m/s and that indicated by the filled square at  $|U| = 12$  m/s ( $= 33 \times R_{AB}$   
 156 m/s) in Fig. 2.) Hence, we can conclude that acoustic minor loss is generated in the setup.

157 As previously mentioned, the measured  $\Delta W$  is proportional to the third power of  $|U|$ ;  
 158 hence, we can use Eq. (1), as suggested by Swift and Wakeland<sup>37</sup>. Using the least squares  
 159 method, the gradient of  $g$  of the obtained data is calculated to be  $7.0 \times 10^{-5}$  kg/m. From

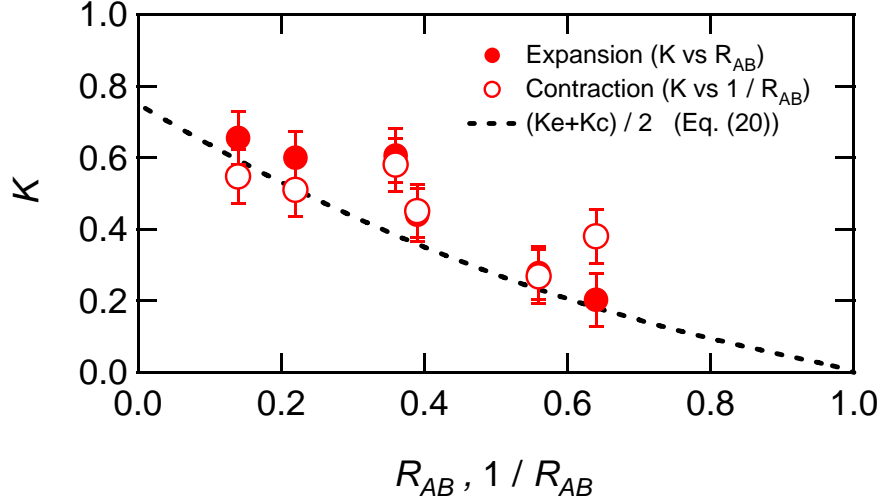
Eq. (1),  $g$  can be related to the acoustic minor loss coefficient  $K$  as follows:

$$K = \frac{3\pi}{2S_i\rho_m}g, \quad (17)$$

where  $S_i$  is the cross-sectional area of the narrower tube and  $S_i = S_A$  for this case; hence  $K = 0.60$  with  $R_{AB} = 0.36$ .

Next, we perform the experiment with several values of  $R_{AB}$  and determine the value of  $K$ . The relationship between  $K$  and  $R_{AB}$  or  $1/R_{AB}$  is shown in Fig. 4. The unfilled symbols indicate the data under the expansion condition ( $R_{AB} < 1$ ) whereas the filled ones indicate the data under the contraction condition ( $R_{AB} \geq 1$ ). It is important to note that when  $R_{AB} > 1$ ,  $1/R_{AB}$  is considered as the horizontal axis instead of  $R_{AB}$ . As shown in Fig. 4, the obtained value of the acoustic minor loss coefficient  $K$  decreases with the increase in  $R_{AB}$  and  $1/R_{AB}$ . The observed dependence of  $K$  on  $1/R_{AB}$  smoothly connects the value of  $K$  numerically predicted by Morris et al.<sup>4</sup> and that experimentally obtained by Doller<sup>6</sup>; Morris et al.<sup>4</sup> reported that when  $1/R_{AB} = 0.01$ ,  $K = 0.9$ , whereas Doller showed that when  $1/R_{AB} = 0.03$ ,  $K = 0.85$ . Furthermore, the data indicated by the unfilled and filled symbols approximately agree with each other; the maximum discrepancy is 0.18. This implies that the minor loss coefficient  $K$  can be set to be the same for abrupt tube expansion as well as contraction.

Next, the minor loss coefficient of this study (oscillatory flow case) and that of the unidirectional flow case are compared. According to the textbook<sup>19</sup>, when fluid flows unidirec-


 FIG. 4. Empirically determined acoustic minor loss coefficient  $K$ .

tionally in a tube, the minor loss coefficient becomes

$$K_e = (1 - R_{AB})^2 \quad (18)$$

$$(R_{AB} < 1)$$

for the expansion condition.

$$K_c = 0.5 \left(1 - \frac{1}{R_{AB}}\right)^{0.75} \quad (19)$$

$$(R_{AB} > 1)$$

for the contraction condition. Because the measured result indicates that  $K$  is the same in

the expansion and contraction cases, we represent the mean of  $K_e$  and  $K_c$  in Fig. 4 by a

dotted line:

$$K = \frac{1}{2} \left(1 - \frac{A_i}{A_j}\right)^2 + \frac{1}{4} \left(1 - \frac{A_i}{A_j}\right)^{0.75} \quad (20)$$

$$(A_i < A_j).$$

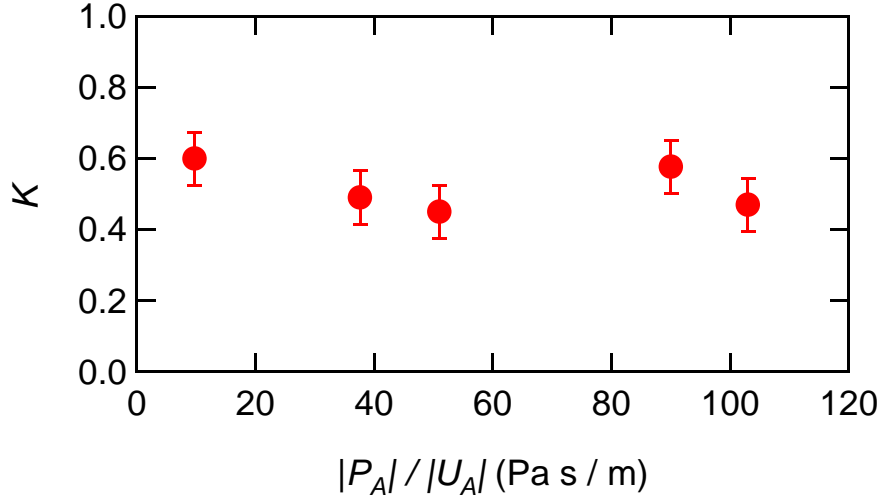


FIG. 5. Acoustic impedance dependence of the minor loss coefficient.

183 This dotted line shows approximate agreement with the obtained experimental data; hence,  
 184 Eq. (20) can be used as an approximation for the acoustic minor loss coefficient  $K$ .

185 *2. Effect of the acoustic impedance and frequency on the acoustic minor loss*  
 186 *coefficient*

187 To investigate the effect of the absolute value of the acoustic impedance on coefficient  $K$ ,  
 188 we measure  $K$  by varying the connecting point, namely,  $L_3$ ; The values of  $L_3$  were set to  
 189 0.3, 0.4, 0.5, 0.6, and 0.7 m. This implies that the connecting point is located between the  
 190 pressure and velocity antinodes. In the experiment,  $R_{AB}$  is maintained at 0.36 and  $\omega/(2\pi)$   
 191 is 161 Hz. The measured  $K$  is plotted as a function of  $|P|/|U|$ , as displayed in Fig. 5.  
 192 The upper limit of  $|P|/|U|$  is determined by the performance of the speaker; when  $|P|/|U|$   
 193 is large, large  $|U|$  is not obtained. In Fig. 5, significant dependence of  $K$  on the value of

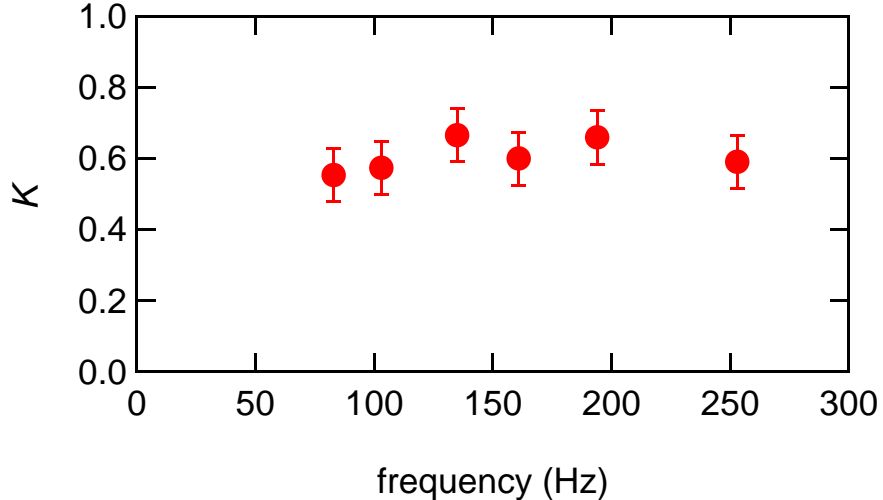


FIG. 6. Frequency dependence of the minor loss coefficient.

194  $|P|/|U|$  is not obtained. This indicates that the acoustic minor loss is governed by the value  
 195 of  $|U|$ , and that the effect of the pressure amplitude  $|P|$  on  $K$  is less.

196 Further, we examine the effect of the frequency,  $\omega/(2\pi)$ , on the value of  $K$ . For a fixed  
 197 value of  $R_{AB}$  ( $= 0.36$ ),  $K$  is measured when the frequency of the acoustic wave is varied  
 198 from 83-253 Hz. For this experiment, the length  $L_3$  of tube B is changed such that the  
 199 connecting point is always fixed in the vicinity of the velocity antinode. The tested values  
 200 of  $L_3$  were 0.3, 0.4, 0.5, 0.6, 0.8 and 1.0 m. The results (Fig. 6) indicate that the frequency  
 201 has no significant effect on the value of  $K$  in the used frequency range.

### 202 C. Effect of tapered tube on the minor-loss reduction

203 To reduce minor loss, a tapered tube with a gradually changing cross-sectional area is  
 204 generally employed<sup>1,5,6,20-22</sup>. In this subsection, we demonstrate the quantitative effect of  
 205 a tapered tube on the reduction of the acoustic minor loss coefficient. As a parameter

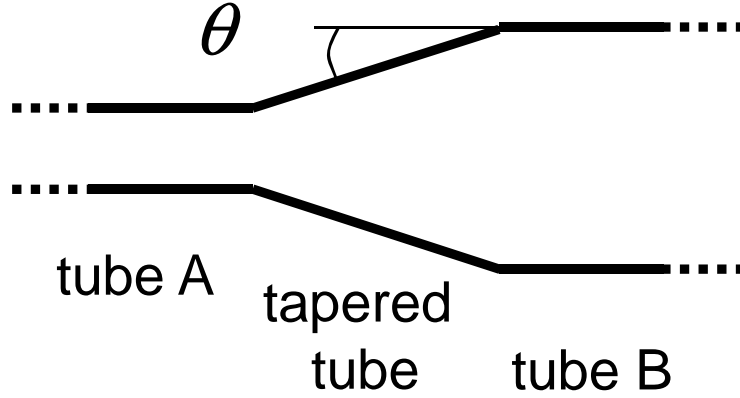


FIG. 7. Schematic of the used tapered tube and the definition of the taper angle  $\theta$ .

206 depicting the tapered tube characteristics, we define the taper angle  $\theta$ , as shown in Fig. 7.  
 207 The radii of tubes A and B are fixed at 12 mm and 20 mm, respectively. The frequency of  
 208 the input acoustic wave is fixed at 161 Hz, and the tapered tube is positioned in the vicinity  
 209 of the velocity antinode.

210 In Fig. 8(a), the evaluated  $K$  is depicted as a function of  $\theta$ . The condition  $\theta = 90^\circ$   
 211 refers to an abrupt area change, whereas  $\theta = 0^\circ$  indicates a straight tube. Note that in this  
 212 evaluation, the effect of the dissipation due to the length of the tapered tube is included  
 213 in  $K$ ; hence,  $K$  will become infinity when  $\theta = 0^\circ$ . However, when  $\theta = 8^\circ$ , the length of  
 214 the tapered tube is 56 mm and the effect of the dissipation due to the length is negligible  
 215 in the conducted experiments. As observed in Fig. 8(a), when  $\theta > 15^\circ$ , the minor loss  
 216 coefficient  $K$  reduces with the decrease in  $\theta$ , and the value of  $K$  at  $\theta = 30^\circ$  becomes less  
 217 than half of that without the tapered tube. Note that the lengths of the tapered tube at  
 218  $\theta = 60^\circ$  and  $30^\circ$  are 4.6 mm and 14 mm, respectively, and are comparable to the radii of  
 219 the tubes. Furthermore, the value of  $K$  at  $\theta = 15^\circ$  is almost equal to that of a straight tube  
 220 within the error margin. Therefore, we can conclude that the use of a tapered tube is an

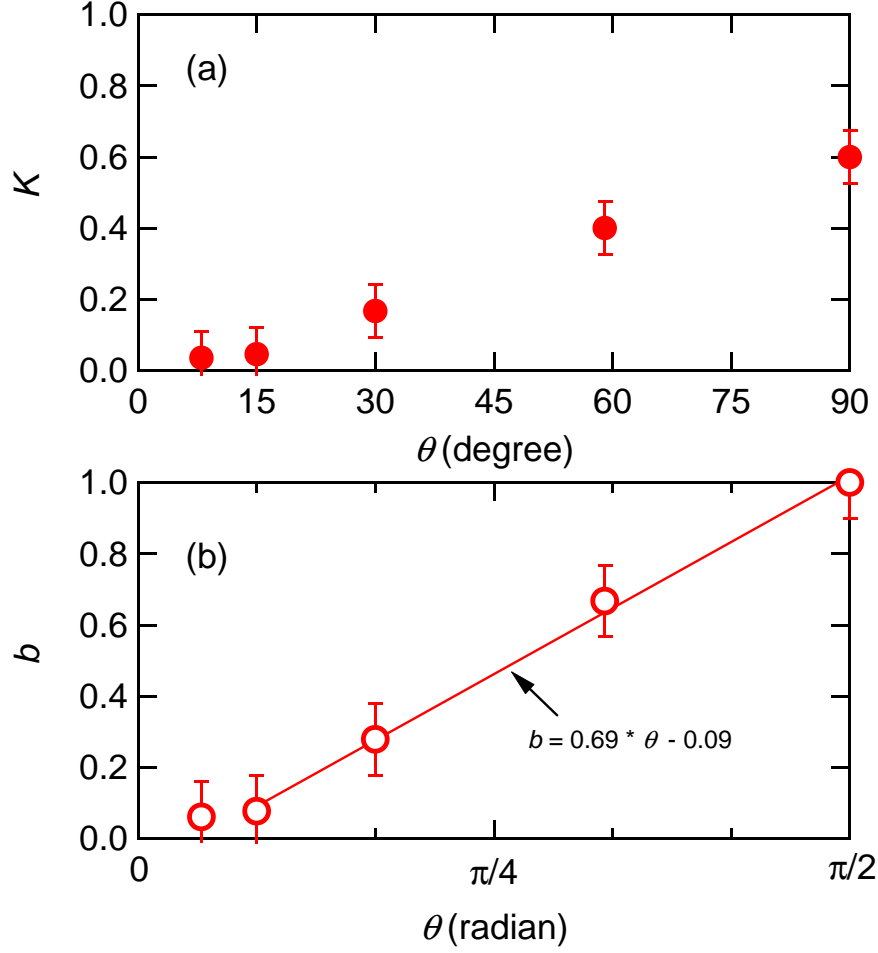


FIG. 8. The taper angle dependence of the (a) minor loss coefficient and (b) normalized coefficient

$$b = K/K_{\theta=\pi/2}.$$

221 effective method for reducing the acoustic minor loss, and that a tapered tube with a length  
 222 comparable to the tube radius can reduce the acoustic minor loss by half.

223 To obtain the approximation of the effect of the taper angle, we introduce the normalized  
 224 coefficient  $b = K/K_{\theta=\pi/2}$  and plot it in Fig. 8(b). As observed in this figure, when  $\pi/2 >$   
 225  $\theta > \pi/12$ ,  $b$  is almost a linear function of  $\theta$  and can be approximately expressed as

$$b(\theta) = 0.69 \times \theta - 0.09. \quad (21)$$

Therefore, we propose an empirical equation to estimate the acoustic minor loss for coupling Eq. (20) and Eq. (21) as follows:

$$K = b(\theta) \times \left( \frac{1}{2} \left( 1 - \frac{A_i}{A_j} \right)^2 + \frac{1}{4} \left( 1 - \frac{A_i}{A_j} \right)^{0.75} \right) \quad (22)$$

(  $A_i < A_j, \pi/12 < \theta < \pi/2$ ).

## V. VALIDATION OF THE OBTAINED EMPIRICAL $K$

In order to validate Eq. (22), we perform an experiment using pressurized helium as a working fluid. The experimental setup is composed of a power source (thermoacoustic engine), resonator, and tank, as shown in Fig. 9. The setup is filled with helium at a time-averaged pressure of 0.8 MPa or 1.1 MPa. The inner radii the neck tube and the tank are 49 mm and 195 mm, respectively, (Fig. 9); hence, ratio  $A_i/A_j = 0.063$ . The taper angle  $\theta$  is estimated using CAD data and is  $33^\circ$ . Note that because welding is used to connect the neck tube to the tapered tube, the connecting point is not sharp. Substituting these values in Eqs. (21) and (22), we obtain  $K = 0.21$ .

Pressure sensors are mounted on the wall of the resonator and the acoustic power flowing to the tank is measured when the velocity amplitude is varied. All this acoustic power is dissipated in the tank mainly at the point where the cross-section changes. The power source generates an acoustic wave of  $59 \pm 1$  Hz, and the velocity antinode is found to be located near the tank inlet.

The measured acoustic power with 0.8 MPa helium and that with 1.1 MPa helium, respectively, are depicted by unfilled and filled squares in Fig. 10 as a function of the cubic of the velocity amplitude, respectively. The dissipated power is approximately proportional

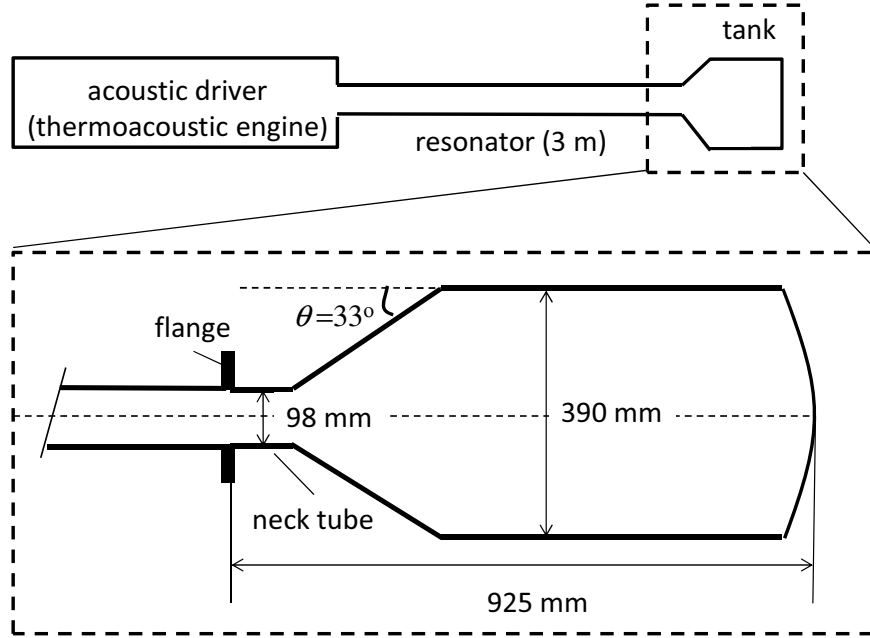


FIG. 9. Schematic illustration of the experimental setup for validation.

245 to the cubic of  $|U|$  and the time averaged pressure, as expected based on Eq. (1). Using  
 246  $K = 0.21$  and Eq. (1), we estimate the minor loss, and display it in Fig 10 using solid  
 247 and dotted lines. In this figure, the estimated loss is in good agreement with the measured  
 248 power. Therefore, we conclude that Eq. (22) can be used for estimating the acoustic minor  
 249 loss.

## 250 VI. CONCLUSION

251 In this study, the minor loss that occurs at abrupt changes in the tube cross-section  
 252 was measured, and the minor loss coefficient  $K$  was experimentally determined. It was  
 253 established that  $K$  is independent of the frequency and acoustic impedance, and that the  
 254 dependence of  $K$  on the cross-sectional area ratio can be expressed by an equation based  
 255 on the minor loss coefficient for unidirectional flow. Furthermore, the reduction effect of a

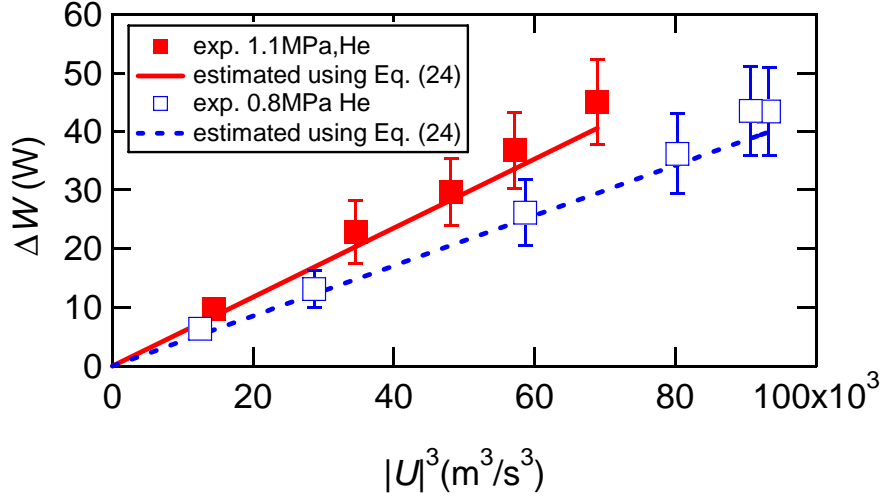


FIG. 10. Measured acoustic power and estimated minor loss.

256 tapered tube on  $K$  was investigated. When the taper angle  $\theta = 15^\circ$ ,  $K$  was reduced to 10%  
 257 of that without the tapered tube. An empirical model was proposed based on the obtained  
 258 data, in addition. The proposed model was validated using a system filled with pressurized  
 259 helium; the estimated and experimental data were in good agreement.

## 260 ACKNOWLEDGMENTS

261 This work was supported by JSPS KAKENHI Grant Number 19H02607.

## 262 REFERENCES

- 263 <sup>1</sup>A. Petculescu and L. Wilen, “Oscillatory flow in jet pumps: Nonlinear effects and minor  
 264 losses”, *J. Acoust.Soc. Am.* **113**, 1282–1292 (2003).
- 265 <sup>2</sup>B. Smith and G. W. Swift, “Power dissipation and time-averaged pressure in oscillating  
 266 flow through a sudden area change”, *J. Acoust. Soc. Am.* **113**, 2455–2463 (2003).

- 267 <sup>3</sup>R. S. Wakeland and R. M. Keolian, “Influence of velocity profile nonuniformity on minor  
268 losses for flow existing thermoacoustic heat exchangers”, *J. Acoust. Soc. Am.* **115**, 2071–  
269 2074 (2004).
- 270 <sup>4</sup>P. J. Morris, S. Boluriaan, and C. M. Shieh, “Numerical simulation of minor loss due to  
271 a sudden contraction and expansion in high amplitude acoustic resonators”, *Acta Acust.*  
272 *united Ac.* **90**, 393–409 (2004).
- 273 <sup>5</sup>C. V. King and B. L. Smith, “Oscillating flow in a 2-d diffuser”, *Exp. Fluids* **51**, 1577–1590  
274 (2011).
- 275 <sup>6</sup>A. J. Doller, “Acoustic minor losses in high amplitude resonators with sigle-sided junc-  
276 tions”, Pennsylvania State University, 2004.
- 277 <sup>7</sup>H. Tijdeman, “On the propagation of sound waves in cylindrical tubes”, *J. Sound Vib.*  
278 **39**, 1–33 (1975).
- 279 <sup>8</sup>T. Yazaki, Y. Tashiro, and T. Biwa, “Measurements of sound propagation in narrow  
280 tubes”, *Proc. R. Soc. London, Ser. A* **463**, 2855–2862 (2007).
- 281 <sup>9</sup>T. Biwa, Y. Tashiro, H. Nomura, Y. Ueda, and T. Yazaki, “Experimental verification of  
282 a two-sensor acoustic intensity measurement in lossy ducts”, *J. Acoust. Soc. Am.* **124**,  
283 1584–1590 (2007).
- 284 <sup>10</sup>Y. Ueda and N. Ogura, “Measurement of acoustic dissipation occurring in narrow channels  
285 with wet wall”, *J. Acoust. Soc. Am.* **145**, 71–76 (2019).
- 286 <sup>11</sup>Dan Mapes-Riordan, “Horn Modeling with conical and cylindrical transmission-line ele-  
287 ments”, *J. Audio. Eng. Soc.* **41**, 471–484 (1993).

- 288 <sup>12</sup>N. Rott, “Damped and thermally driven acoustic oscillations”, *Z. Angew. Math. Phys.* **20**,  
 289 230–243 (1969).
- 290 <sup>13</sup>G. W. Swift, *Thermoacoustics: A Unifying Perspective for Some Engines and Refrigerators*  
 291 (Acoustical Society of America, Pennsylvania) (2002).
- 292 <sup>14</sup>A. Tominaga, *Fundamental Thermoacoustics* (Uchidarokakumo, Tokyo) (1998).
- 293 <sup>15</sup>Y. Ueda and C. Kato, “Stability analysis for spontaneous gas oscillations thermally induced  
 294 in straight and looped tubes”, *J. Acoust. Soc. Am.* **124**, 851–858 (2008).
- 295 <sup>16</sup>T. Biwa and T. Yazaki, “Observation of energy cascade creating periodic shock waves in  
 296 a resonator”, *J. Acoust. Soc. Am.* **127**, 1189–1192 (2010).
- 297 <sup>17</sup>M. Ohmi and M. Iguchi, “Critical Reynolds number in an oscillating pipe flow”, *Bulletin*  
 298 *of the JSME* **25**, 165–172 (1982). Merkli
- 299 <sup>18</sup>P. Merkli and H. Thomann, “Transition to turbulence in oscillation pipe flow”, *J. Fluid*  
 300 *Mech.* **68**, 567–575 (1975).
- 301 <sup>19</sup>I. Idelchik, *Handbook of hydraulic resistance* (Jaico publishing house, Mumbai) (2003).
- 302 <sup>20</sup>S. Backhaus and G. W. Swift, “A thermoacoustic Stirling engine”, *Nature* **399**, 335–338  
 303 (1999).
- 304 <sup>21</sup>J. P. Oosterhuis, S. Buhler, D. Wilcox, and T. H. Van der Meer , “A numerical investigation  
 305 on the vortex formation and flo separation of the oscillatory flow in jet pumps”, *J. Acoust.*  
 306 *Soc. Am.* **137**, 1722–731 (2015).
- 307 <sup>22</sup>J. P. Oosterhuis, S. Buhler, D. Wilcox, and T. H. Van der Meer , “Jet pumps for thermo-  
 308 acoustic applications: Design guidelines based on a numerical parameter study”, *J. Acoust.*

309 Soc. Am. **138**, 1991–2002 (2015).